Macromolecular Research, Vol. 11, No. 4, pp 250-255 (2003)

Effect of the Photosensitizer on the Photorefractive Effect Using a Low T_g Sol-Gel Glass

Dong Hoon Choi*, Woong Gi Jun, Kwang Yong Oh, Han Na Yoon, and Jae Hong Kim

College of Environment and Applied Chemistry, Institute of Natural Sciences, Kyung Hee University, Yongin, Kyungki 449-701, Korea

Received Dec. 18, 2002; Revised May 26, 2003

Abstract: We prepared the photorefractive sol-gel glass based on organic-inorganic hybrid materials containing a charge transporting molecule, second-order nonlinear optical (NLO) chromophore, photosensitizer, and plasticizer. Carbazole and 2-{4-[(2-hydroxy-ethyl)-methyl-amino]-benzylidene}-malononitrile were reacted with isocyanato-triethoxy silane and the functionalized silanes were employed to fabricate the efficient photorefractive media including 2,4,7-trinitrofluorenone (TNF) to form a charge transfer complex. The prepared sol-gel glass samples showed a large net gain coefficient and high diffraction efficiency at a certain composition. As the concentration of photosensitizer increased, the photorefractive properties were enhanced due to an increment of charge carrier density. Dynamic behavior of the diffraction efficiency was also investigated with the concentration of the photosensitizer.

Keywords: sol-gel, photorefractivity, two-beam coupling, degenerated four wave mixing, gain coefficient, diffraction efficiency.

Introduction

Photorefractive (PR) materials have much attention as principal candidates for the medium of real time holographic display.[1-4] Organic PR materials are considered to be very much promising since they possess unique advantages such as the highest figure of merit, structural flexibility, ease of fabrication, low dielectric constant, and low cost compared to inorganic PR crystalline materials.[5-10]

The PR effect can be observed in a bifunctional organic material system that exhibits photoconductivity and electro-optic properties. The charge carriers generated in the bright regions of a spatially modulated light migrate by thermal diffusion or applied electric field and become trapped in the dark regions, resulting in the formation of a nonuniform space charge field. The modulation of the refractive index is caused, *via* Pockels effect, by the induced internal space charge field.

Among many kinds of fabrication method for PR samples, organic and inorganic hybrid materials prepared through sol-gel process have been attractive due to simple and easy method.[11-13] Compared to organic polymeric systems, it can be prepared by simple hydrolysis and condensation process at a relatively low temperature using the functionalized silanes and various kinds of guest molecules. Silicon trialkoxide derivatives can be simply designed to bear a functional group in one arm of silicon through a flexible spacer. The resultant chemical structure of the matrix used herein is quite similar to that of the functional side-chain copolymers. It is advantageous that the composition in the sol-gel glass was controlled accurately. The synthesis of the functionalized silane is also very easy and it can give us a well-defined bulk matrix containing the desired amount of the functional molecules.

In this work, we fabricated the sol-gel glass samples varying the concentration of the photosensitizer for showing the variation of photorefractive effect and reported fairly high net gain and high diffraction efficiency with the sample bearing a high concentration of photosensitizer. The dynamic behaviors of the diffraction efficiency in three samples were also compared to investigate the effect of the concentration of the photosensitizer.

Experimental

The structures of the functional silane compounds that were employed to prepare the PR composite were illustrated in Figure 1. SG-Cz is the silane bearing a carbazole unit and SG-MN bears a second-order nonlinear optical (NLO) chromophore. For preparing the viscous solution to fabricate the thick film, SG-Cz and SG-MN were dissolved in tetrahydrofuran (THF) in the presence of H_2O and hydrochloric

*e-mail : dhchoi@khu.ac.kr

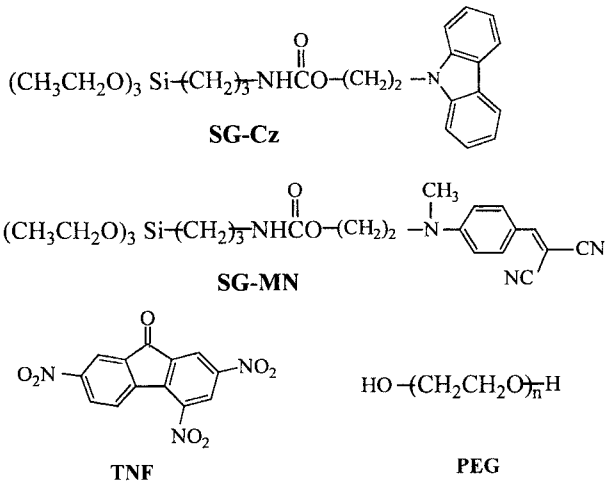

Figure 1. Chemical structures of the compounds used in the photorefractive sol-gel glass.

acid. The molar composition of the solution is as follows: SG-Cz/SG-MN : H_2O : HCl : THF = 1 : 6 : 0.01 : 4. A proper amount of polyethylene glycol (PEG) was added to plasticize the matrix. The solution was filtered through acrodisc syringe filter (Millipore 0.2 μm) and then cast on the indium tin oxide (ITO) pre-coated glass. The film was dried overnight at 80 °C under vacuum. After the solvent was removed completely, another ITO glass was placed on the top of the film and then pressed down at 80 °C using the 75 μm polyimide film as a spacer to get the sandwich device for the two-beam coupling (2BC) and the degenerated four wave mixing (DFWM) experiments. UV-Vis absorption spectroscopy was performed on a Hewlett Packard 8453 spectrophotometer (PDA type, λ = 190-1,100 nm).

Photorefractivity. Measurement of photorefractive property was conducted with a 2BC and a DFWM technique. In a 2BC experiment, A 633 nm wavelength He-Ne laser was incident on the sample and two p-polarized laser beams with an equal intensity of 60.7 mW/cm^2 were coupled on the sample to write the refractive index grating. The incident-crossing angle of the beams is 6° and the film normal was tilted at an angle of 50° with respect to the symmetric axis of the two writing beams. The transmitted intensities of both beams were detected using two calibrated photodetectors (Newport, Model 1815-C, Photodiode, 818-SL) and were recorded with a personal computer.

For the DFWM experiment, two s-polarized beams with the 70 mW/cm^2 were used as writing beams and a p-polarized reading beam with the intensity of 1 mW/cm^2 counterpropagated to one of the writing beams. The normal of the sample surface was tilted 50° with respect to the symmetric axis of the two intersected beams and the angle between the two-coupled beams was set to be 20°. The diffraction efficiency was determined by the ratio of the intensity of the diffracted signal to that of the incident reading beam and the dynamic behavior was also observed.

Results and Discussion

The prepared SG-MN and SG-Cz are well soluble in THF, dichloromethane, acetone, dimethylformamide, pyridine etc. The structures of the functional silicon alkoxide compounds that were employed to prepare the PR sample were illustrated in Figure 1 including the photosensitizer and the plasticizer used in this study. Polyethylene glycol (M_n ~ 600) plays an important role to improve the miscibility preventing from phase separation.[14] The composition of the PR matrix was adjusted to be 30 : 60 : 10 of SG-Cz, SG-MN, and polyethylene glycol respectively. TNF was also used as a photocharge generating sensitizer to be doped into the sample and the concentration was varied to be 0 (Sample I), 1 (Sample II), and 2 wt% (Sample III).

Before measuring the PR property of the sol-gel glass, we firstly recorded the UV-Vis absorption spectra of three PR samples. In Figure 2, we investigated the absorption property due to formation of charge transfer (CT) complex of three samples containing different concentration of TNF. All samples showed small and broad absorption around 640-700 nm. TNF concentration has a significant effect on the photoconductivity and the density of charge transfer complex unit, and therefore the absorption coefficient, α increased with the doping concentration, as did the charge carrier generation rate. As the concentration of the photosensitizer increases, the absorption coefficient appeared to be higher than the others. Therefore, the sample III containing highest concentration of TNF showed highest absorption coefficient (α = 66.6 cm^{-1}) at 633 nm. We can expect the generation of higher density of charge carrier in the sample III under irradiation for an identical period.

Photorefractivity measurements were conducted with a 2BC and a DFWM techniques after applying d.c. voltage for 10 min for saturated molecular orientation. A 633 nm

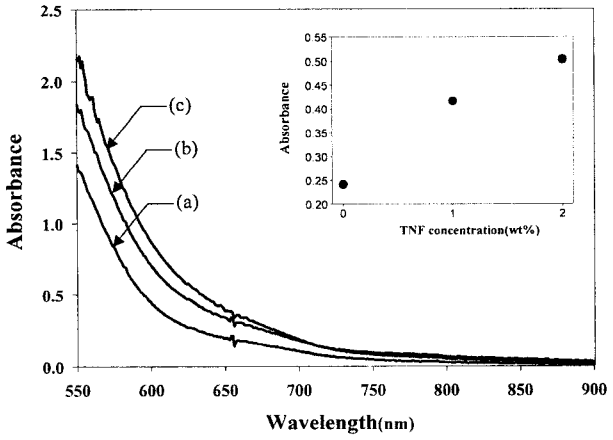

Figure 2. UV-Vis absorption spectra of three samples. (a) sample I, (b) sampl II, and (c) sample III.

wavelength He-Ne laser was incident on the sample. In the 2BC measurement, the change in the transmitted intensity of either of the two writing beams is recorded as the other beam is switched on and a PR grating is formed. One of writing beams is partially diffracted in the direction of the other writing beam through the PR grating. An asymmetric change in the intensities of the two writing beams can only occur from an index of refraction grating which is phase shifted relative to the intensity grating. Thus the asymmetric change of intensity of the two writing beams as the grating is written, is a clear evidence of the PR effect. Resulting from the two-beam coupling experiment, optical coupling gain coefficient (Γ) was calculated according to the equation (1).

$$\Gamma = (1/L) \times \ln [\gamma/(2 - \gamma)] \quad (1)$$

where L is the optical path for the amplified beam and γ is the beam coupling ratio (the ratio of the signal intensities with and without pump beam). The calculated gain coefficients due to the asymmetric energy transfer between the two beams are shown in Figure 3. The sample III comprised much higher concentration of the photosensitizer and showed higher optical coupling gain coefficient over whole range of the applied electric field. The maximum net gain was observed to be higher than ~230 cm^{-1} in the sample III since the absorption coefficient is measured to be 66.6 cm^{-1}. In these sol-gel glasses, the effect of the concentration of the photosensitizer was also found pronounced accompanying with the effect of the NLO and charge transporting molecules.

We have investigated the grating buildup dynamics at 632 nm in terms of the diffraction efficiency. In the DFWM experiment, the diffraction efficiency (η) was determined by the ratio of the intensity of the diffracted signal to that of the incident reading beam. We also observed the growing and decaying behavior of the diffraction efficiency using the samples containing a different concentration of TNF. Figure 4 shows the electric field dependence of the diffraction efficiency. The diffraction efficiency increased with the applied electric field and the maximum diffraction efficiency (η = 50%) of sample IIII was achieved at 80 V/μm. It may be attributed to the highest concentration of the generated charge carriers which can transport/trap and induce the higher amplitude of the space charge field. In sample III, higher density of trapped holes induces the higher space charge field to induce the change of the refractive index nonlocally. Additionally, the field dependence of the steady-state diffraction efficiency of the three samples was well described by the Kogelnik coupled-wave model.[15] We also calculated refractive index modulation (Δn) according to the theory, which was shown as an inset in Figure 4.

The speed of PR grating buildup can be determined by the photo-induced generation efficiency of the charge carriers by the migration and trapping dynamics of these charges or by the rotational mobility of the chromophores. The dynamics of the holographic grating formation were studied by measuring the time constants of the grating formation in the DFWM experiment. In Figure 5, we could observe the rising behavior of the diffraction efficiency in three samples (E = 80 V/μm). Once the photosensitizer is added, the grating growth rate becomes faster than that without photosensitizer. The photosensitivity was improved by increasing the TNF concentration. As we observed in Figure 5, the sample III with highest concentration of TNF showed faster rising behavior and higher diffraction efficiency at a glance. Quantitative information about the grating growth can be obtained by an empirical double exponential function of the following equation (2) fitted to the data of diffraction efficiency.

$$\eta(t) = \eta_o [1 - (a \exp(-t/\tau_1) + (1-a) \exp(-t/\tau_2))]^2 \quad (2)$$

where a, τ_1, and τ_2 are the three fitting parameters. η_o is the steady state diffraction efficiency. The fast response time

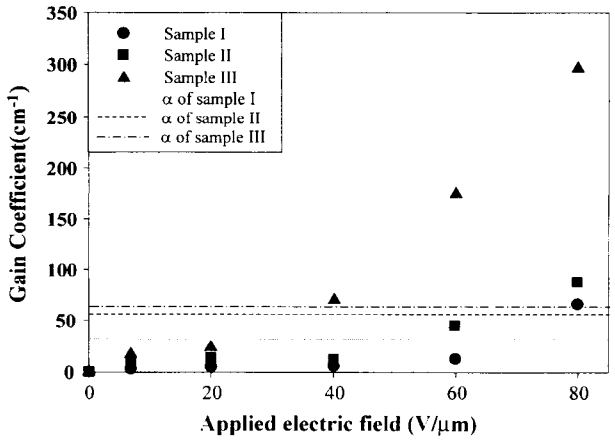

Figure 3. Optical gain coefficient as a function of the applied electric field.

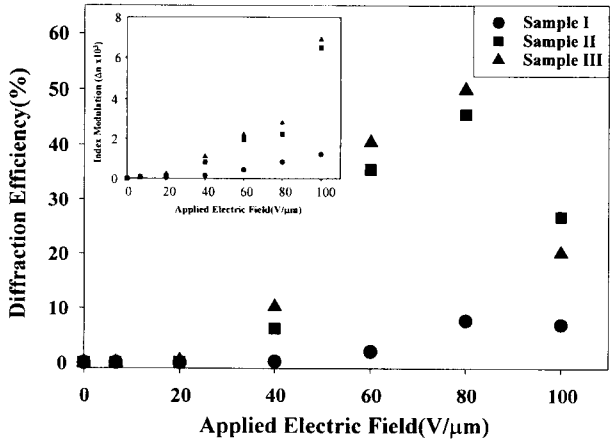

Figure 4. Diffraction efficiency as a function of the applied electric field.

(τ_1) of the diffraction efficiency is indicated by the first term of the equation. Such a fast response time may be attributed to large charge carrier mobility. In Figure 6, we described the dependence of the fast time constants, indicating the rising speed of the space charge field with the square root of the applied electric field. Sample III showed faster grating formation than the other two samples. Highest speed of the space charge field build up can be expected to induce highly resolved diffraction grating in this sample. Once the holes were transported through the medium, they will be trapped in a certain energy level. The holes are transported from the HOMO level of SG-Mn to the HOMO level of SG-Cz. Finally, they are trapped in a certain energy level which place in the middle of the HOMO and LUMO of SG-Cz and SG-Mn. The hole trapping population in sample III is expected to be much higher than the others because the concentration of the trapped charge carrier could be larger and it can induce higher trapping probability of transported holes. As the applied electric field is higher, the carrier is transported very fast and trapped to give a space charge field with a fast rate. Shortly, photocharge carrier generation plays a very important role in the dynamic behavior of the diffraction efficiency that is closely related to the space charge field buildup.

After the diffraction light intensity was almost saturated (E = 80 V/μm), we blocked one beam. Then, we observed the decaying behavior of the diffraction efficiency in three samples.[16] In Figure 7, the decaying behaviors have some difference between the samples with different concentration of the photosensitizer. The decaying behavior is mainly dependent on the decrease of the space charge field and reorientation of the chromophore. It can be governed by the rate of detrapping of the trapped holes and the rate of chromophore relaxation. After fitting the diffraction efficiency during decaying to the double exponential decaying function (3), we could calculate the fast decaying time constant described in Figure 8.[17]

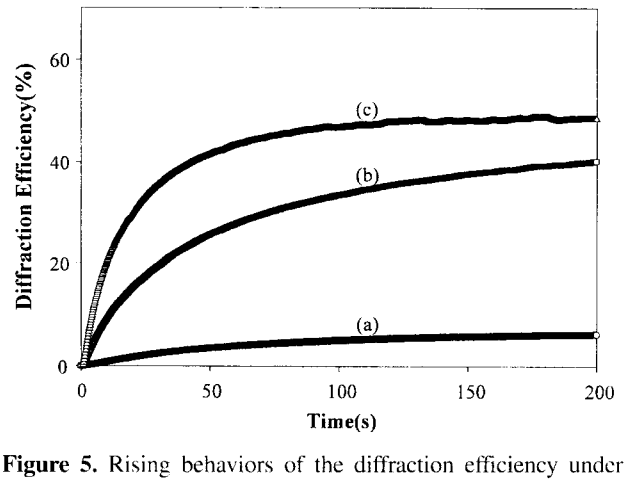

Figure 5. Rising behaviors of the diffraction efficiency under 80 V/μm. (a) sample I, (b) sample II, and (c) sample III.

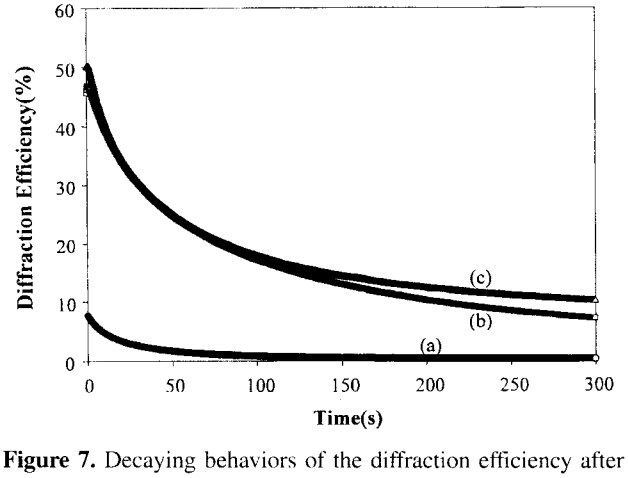

Figure 7. Decaying behaviors of the diffraction efficiency after blocking one beam (E = 80 V/μm). (a) sample I, (b) sample II, and (c) sample III.

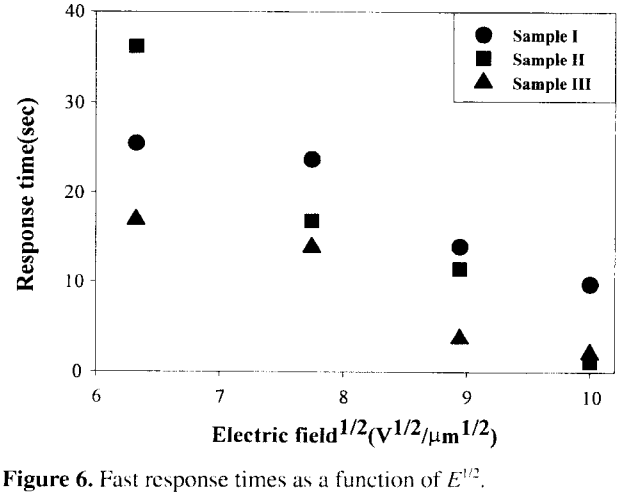

Figure 6. Fast response times as a function of $E^{1/2}$.

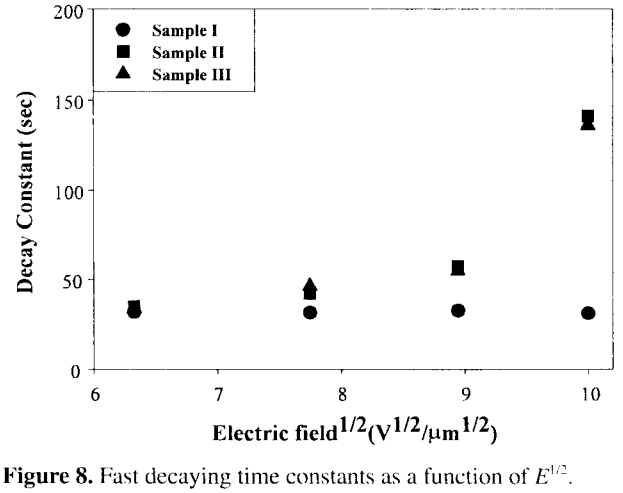

Figure 8. Fast decaying time constants as a function of $E^{1/2}$.

$$\eta(t) = \eta_o [(a' \exp(-t/\tau_3) + (1-a') \exp(-t/\tau_4))]^2 \quad (3)$$

where τ_3 and τ_4 are the fast and slow decay time constants respectively. This function has been applied for various PR polymers to quantify the time scale of the erasure process.[18-20]

As the applied electric field is higher, the decaying time constant is larger. This is unusual phenomenon compared to the decaying behavior of the diffraction efficiency in the other photorefractive polymers. We can explain this phenomenon by the following way although no spectroscopic evidence can be provided in this report. During the writing of the grating, the NLO chromophore oriented to the direction of the combined field of the external dc field and the spatially periodic space charge field. During decaying the diffraction efficiency, the reoriented chromophore randomized to their original position without periodic electric field. In these sol-gel materials, specific interaction through hydrogen bond between carbamate groups in SG-MN and SG-Cz can be expected. After reorientation of the chromophore, new hydrogen bond formation can occur in a new geometrical way. Therefore, as the dc applied field is higher and the more holes can be trapped to induce a larger amplitude of the space charge field, high poled order can be achieved nonlocally so that the density of hydrogen bond may increase.

In order to confirm this unusual behavior indirectly, we did measure the electric field induced birefringence of the PR sample. He-Ne laser ($\lambda = 633$ nm, $I = 0.5$ mW/cm^2) was used as a probe beam and the incident angle was set to be 45°. We measured the transmitted light intensity under applying the dc field with crossed polarizers(see Figure 9). As we expected, the light intensity increased and reached to the asymptotical value after turning on the electric field. Then we turned off the field to monitor the decaying behavior of the light intensity. Using the thickness of the sample, we converted the transmitted light intensity to the birefringence.

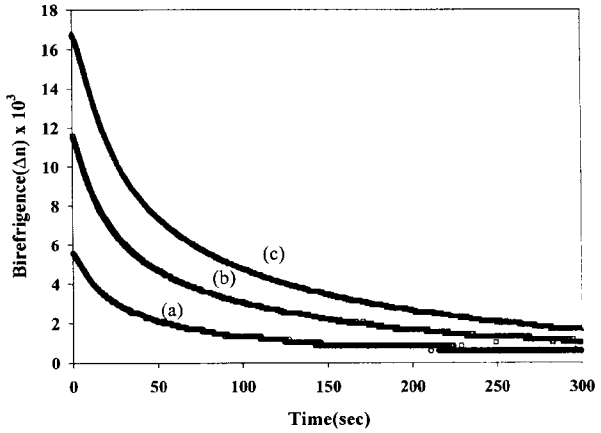

Figure 9. Decaying behavior of the electric field induced birefringence of the sample II. Poling field: (a) 40 V/μm, (b) 60 V/μm, and (c) 80 V/μm.

In the experiment to observe the decrease of the diffraction efficiency, we blocked the one beam, which implys the removal of the space charge field to induce the electro-optic effect. The decaying behavior of the diffraction efficiency under one beam irradiation is relatively comparable to the decaying behavior of the birefringence without dc electric field. That can explain the unique randomization of the alignment of the poled chromophore. We selected the sample II that contains 1% of TNF for this experiment. The applied dc field was varied from 40 to 80 V/μm. The decaying data were fitted to the single exponential equation (4).

$$\Delta n(t)/\Delta n(0) = \exp(-k\,t) + R \quad (4)$$

where k is the rate constant and R is the residue of the

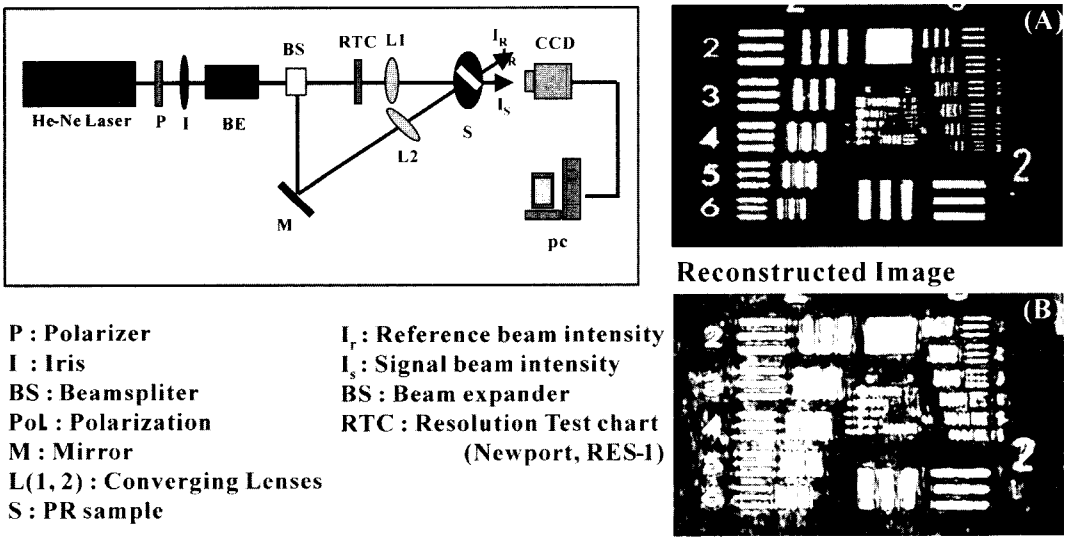

Figure 10. Optical setup and photographs of (A) original image transmitted through the sample III and (B) the reconstructed hologram image ($E = 80$ V/μm).

birefringence after long term decay.

Under calculation of the parameters, we could obtain the rate constant of the birefringence decay. The rate constants of 0.0193, 0.0168, and 0.0162 sec^{-1} were obtained after applying the electric field of 40, 60, and 80 V/μm, respectively. This means that the relaxation of the chromophore alignment is retarded, as the poling dc field is higher. Resultantly, high orientation stability of the chromophore provides the slow decaying behavior of the diffraction efficiency even after blocking the one writing beam. Resultantly, high orientation stability of the chromophore provides the slow decaying behavior of the diffraction efficiency even after blocking the one writing beam.

The potential of PR sol-gel sample (e.g. Sample III) was evaluated for a holographic recording using 75 μm thick sandwich sample. Figure 10(A) is the original target image through the sol-gel glass sample. The image was recorded at the external applied field of 80 V/μm and the stored image is reconstructed by illuminating of the probe beam. In Figure 10(B), the reconstructed hologram image was illustrated and the image can be erased by irradiation of the reference beam blocking the objective beam. This results in the possibility of the sol-gel sample applicable to the holographic recording medium although contrast and resolution should be improved furthermore.

Conclusions

The photorefractive properties of a new series of sol-gel composite materials have been presented. Photoinduced charge generation is facilitated by doping a photosensitizer, TNF. Two miscible molecules such as SG-Cz and SG-MN provide the charge transporting and the second order NLO properties. Resulting from the 2BC and DFWM experiment, sample III with the highest concentration of photosensitizer showed best performance of PR property. Resulting from the dynamic behavior of the diffraction efficiency, the fast response time, τ_1 was found to be affected by the rate of formation of the space charge field governed by the density of photoinduced charge carrier and trapping probability. The general trend of a faster response time can be observed as the applied electric field is increased. Also, we stored the holographic information successfully using the sol-gel PR sample (e.g. Sample III).

Acknowledgements. This research was supported by the Korea Science and Engineering Foundation (contract No. R01-2000-000-00338-0). Dr. Jae Hong Kim particularly acknowledges the financial support from Korea Research Foundation Grant (KRF-2001-005-D00004).

References

(1) B. L. Volodin, R. Sandalphon, K. Meerholz, B. Kippelen, N. V. Kukhtarev, and N. Peyghaambarian, *Opt. Eng.*, **34**, 2213 (1995).
(2) C. J. Chang, W. T. Whang, C. C. Hsu, Z. Y. Ding, K. Y. Hsu, and S. H. Lin, *Macromolecules*, **32**, 5637 (1999).
(3) S. J. Strutz and L. M. Hayden, *Appl. Phys. Lett.*, **74**, 2749 (1999).
(4) A. Goonesekera, D. Wright, and W. E. Moerner, *Appl. Phys. Lett.*, **76**, 3358 (2000).
(5) D. V. Steenwinckel, C. Engels, E. Gubbelmans, E. Hendrickx, C. Samyn, and A. Persoons, *Macromolecules*, **33**, 4074 (2000).
(6) H. Moon , J. Hwang, N. Kim, and S. Y. Park, *Macromolecules*, **33**, 5116 (2000).
(7) K. Okamoto, T. Nomura, S. H. Park, K. Ogino, and H. Sato, *Chem. Mater.*, **11**, 3279 (1999).
(8) M. S. Ho, C. Barrett, J. Paterson, M. Esteghamatian, A. Natansohn, and P. Rochon, *Macromolecules*, **29**, 4613 (1996).
(9) Z. Peng, A. R. Gharavi, and L. Yu, *J. Am. Chem. Soc.*, **119**, 4622 (1997).
(10) J. Sohn, J. Hwang, S. Y. Park, J. K. Lee, J. H. Lee, J. S. Chang, G. J. Lee, B. Zhang, and Q. Gong, *Appl. Phys. Lett.*, **77**, 1422 (2000).
(11) B. Darracq, F. Chaput, K. Lahlil, J. P. Boilot, Y. Levy, V. Alain, L. Ventelon, and M. B. Desce, *Optical Mater.*, **9**, 265 (1998).
(12) G. H Hsiue, W. J. Kuo, C. H. Lin, and R. J. Jeng, *Macromol. Chem. Phys.*, **17**, 2336 (2000).
(13) B. Darracq, M. Canva, F. Chaput, J. P. Boilot, D. Riehl, Y. Levy, and A. Brun, *Appl. Phys. Lett.*, **70**, 292 (1997).
(14) D. H. Choi, H. T. Hong, W. G. Jun, and K. Y. Oh, *Opt. Mater.*, **21**, 373 (2002).
(15) H. Kogelnik, *Bell. Syst. Tech. J.*, **48**, 2909 (1969).
(16) H. Ono, T. Kawamura, N. M. Frias, K. Kitamura, N. Kawatsuki, H. Norisada, and T. Yamamoto, *J. Appl. Phys.*, **88**, 3853 (2000).
(17) Y. Cui, B. Swedek, N. Cheng, J. Zieba, and P. N. Prasad, *J. Appl. Phys.*, **85**, 38 (1999).
(18) S. M. Silence, R. J. Twieg, G. C. Bjorklund, and W. E. Moerner, *Phys. Rev. Lett.*, **73**, 2047 (1994).
(19) B. E. Jones, S. Ducharme, M. Liphardt, A. Goonesekera, J. M. Takacs, L. Zhang, and R. Athlaye, *J. Opt. Soc. Am. B.*, **11**, 1064 (1994).
(20) S. M. Silence, J. C. Scott, J. J. Stankus, W. E. Moerner, C. R. Moylan, G. C. Bjorklund, and R. J. Tweig, *J. Phys. Chem.*, **99**, 4096 (1995).